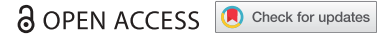


REPORTS



## Co-engaging CD47 and CD19 with a bispecific antibody abrogates B-cell receptor/CD19 association leading to impaired B-cell proliferation

Eric Hatterer<sup>\*a</sup>, Leticia Barba<sup>\*a</sup>, Nelly Noraz<sup>ib</sup>, Bruno Daubeuf<sup>a</sup>, Jean-Pierre Aubry-Lachainaye<sup>ibc</sup>, Benoit von der Weid<sup>a</sup>, Françoise Richard<sup>a</sup>, Marie Kosco-Vilbois<sup>a</sup>, Walter Ferlin<sup>ib</sup>, Limin Shang<sup>#a</sup>, and Vanessa Buatois<sup>#a</sup>

<sup>a</sup>Exploratory Sciences, NovImmune SA, Plan les Ouates, Switzerland; <sup>b</sup>INSERM U1217, Institut NeuroMyoGène, Lyon, University Claude Bernard Lyon 1, Lyon, France; <sup>c</sup>Flow cytometry core facility, Faculty of Medicine, Geneva, Switzerland

### ABSTRACT

CD19 is a B cell-specific receptor that regulates the threshold of B cell receptor (BCR)-mediated cell proliferation. A CD47xCD19 bispecific antibody (biAb) was generated to target and deplete B cells via multiple antibody-mediated mechanisms. Interestingly, the biAb, constructed of a CD19 binding arm and a CD47 binding arm, inhibited BCR-mediated B-cell proliferation with an effect even more potent than a CD19 monoclonal antibody (mAb). The inhibitory effect of the biAb was not attributable to CD47 binding because a monovalent or bivalent anti-CD47 mAb had no effect on B cell proliferation. Fluorescence resonance energy transfer analysis demonstrated that co-engaging CD19 and CD47 prevented CD19 clustering and its migration to BCR clusters, while only engaging CD19 (with a mAb) showed no impact on either CD19 clustering or migration. The lack of association between CD19 and the BCR resulted in decreased phosphorylation of CD19 upon BCR activation. Furthermore, the biAb differentially modulated BCR-induced gene expression compared to a CD19 mAb. Taken together, this unexpected role of CD47xCD19 co-ligation in inhibiting B cell proliferation illuminates a novel approach in which two B cell surface molecules can be tethered, to one another in order, which may provide a therapeutic benefit in settings of autoimmunity and B cell malignancies.

### ARTICLE HISTORY

Received 2 October 2018  
Revised 22 November 2018  
Accepted 5 December 2018

### KEYWORDS

Antibody therapy; B cell proliferation; BCR signaling; CD19; receptor clustering

### Introduction

The survival and proliferation of mature B cells is contingent on B cell receptor (BCR) signaling, with tonic stimulation requisite to cell survival and antigen-mediated signaling obligate for cell activation and proliferation.<sup>1–4</sup> In most B cell lymphomas, BCR expression and tonic BCR signaling has been shown to contribute to tumor progression.<sup>5</sup> As such, strategies aimed at abrogating BCR activation are considered a promising therapeutic strategy in B cell malignancies.<sup>6</sup> For example, drugs that target the BCR signaling pathway, such as ibrutinib and idelalisib, demonstrate therapeutic activity in chronic lymphocytic leukemia (CLL).<sup>6</sup>

BCR activation is a complex process, regulated by several cell surface receptors, including CD21, CD81 and CD19.<sup>7</sup> These receptors form a cell surface complex with the BCR (the ‘BCR signaling complex’) to modulate the threshold of cellular activation. CD19, a B cell-specific member of the immunoglobulin superfamily, is a key component of this complex.<sup>8,9</sup> Expressed during most stages of B cell development until plasma cell differentiation, CD19 positively regulates the intrinsic signaling threshold and serves as a costimulatory molecule for amplifying BCR signaling and downstream B-cell proliferation.<sup>7,8,10,11</sup> Indeed, clustering of the BCR upon antigen binding induces

the migration of CD19 to the BCR within minutes.<sup>9–11</sup> This molecular association allows CD19 to be phosphorylated at various positions (e.g., tyrosine (Y)-391, Y-482, Y-513 and Y-531), and, thus, function as a membrane adaptor protein recruiting phosphoinositide-3 kinase (PI3K), mitogen-activated protein (MAP) kinase and protein kinase B (AKT), which are key mediators of the BCR signaling pathway.<sup>7,12–14</sup> B cells from CD19-deficient mice are hypo-responsive to BCR stimulation *in vitro* and generate relatively modest immune responses *in vivo*.<sup>15,16</sup> B cells from transgenic mice overexpressing CD19 are hyper-responsive to stimulation and present with elevated humoral immune responses when challenged with antigen *in vivo*.<sup>17,18</sup>


Recent clinical results with CD19/CD3 bispecific T cell engager and CD19-CAR-T therapies are a testament to the success of targeting CD19 as a tumor-associated antigen across multiple B cell malignancies.<sup>19</sup> Therapeutic CD19 mAbs have also been shown to inhibit BCR signaling and B-cell proliferation, highlighting that the role of CD19 in BCR activation may also be exploited to target B cells in autoimmunity and cancer.<sup>20–22</sup>

A CD47xCD19 bispecific antibody (biAb) being developed to target the blockade of CD47-SIRPα on B cells for the treatment of B cell lymphoma and leukemia has been shown to be

**CONTACT** Eric Hatterer  [ehatterer@novimmune.com](mailto:ehatterer@novimmune.com)  NovImmune SA, 14 chemin des Aulx, Plan les Ouates 1228, Switzerland

\*Co-first authors

#Co-last authors

 Supplemental data for this article can be accessed on the [publisher's website](#).

© 2019 The Author(s). Published by Taylor & Francis Group, LLC

This is an Open Access article distributed under the terms of the Creative Commons Attribution-NonCommercial-NoDerivatives License (<http://creativecommons.org/licenses/by-nc-nd/4.0/>), which permits non-commercial re-use, distribution, and reproduction in any medium, provided the original work is properly cited, and is not altered, transformed, or built upon in any way.

very potent *in vitro* and *in vivo* at killing target cells derived from various B cell malignancies.<sup>23</sup> Here, we show that this CD47xCD19 biAb produced an unexpected interference with BCR-induced proliferation and signaling via a CD19 dependent mechanism. Binding to CD47 prevented CD19 clustering and impaired CD19 migration to the BCR domain. Gene expression array analysis highlighted that the co-engagement of CD47 and CD19 on B cells modulated a pattern of BCR-induced genes involved in multiple biological processes (e.g., cell signaling, remodeling of the cytoskeleton, inflammation and metabolism). These results thus demonstrate an unreported role of CD47xCD19 co-ligation in modulating the proliferation of CD19+ cells.

## Results

### **Co-engaging CD47 and CD19 inhibits human B-cell proliferation triggered by BCR cross-linking**

Anti-CD19 mAbs have been demonstrated to inhibit B-cell proliferation induced by BCR-dependent stimulation.<sup>20–22</sup> To further understand the effect of CD19 on BCR-mediated B-cell proliferation, the effect of an anti-CD19 mAb with an antibody variant targeting CD19 monovalently was compared. Human primary B-cell proliferation was induced by the combination of anti-BCR/anti-CD40 mAbs and assessed using flow cytometry. In cells pretreated with human IgG1 isotype control, stimulation with anti-BCR/anti-CD40 mAbs increased the percentage of proliferating B cells from a baseline level of 9.4% to 23.2% (Figure 1a), whereas, as expected, a bivalent anti-CD19 mAb at 10 µg/mL significantly reduced the percentage of proliferating B cells to 15.1%. In contrast, the monovalent anti-CD19 mAb used at the same concentration did not affect B-cell proliferation (Figure 1a). Increasing the concentration of the monovalent antibody to 50 µg/mL, a concentration saturating CD19 binding similarly as the CD47xCD19 biAb (Supplementary Figure 1a) still had no effect on BCR-mediated B-cell proliferation (Supplementary Figure 1b). The results demonstrated that bivalent CD19 engagement is required for the inhibitory effect of the anti-CD19 mAb on B-cell proliferation. Interestingly, the CD47xCD19 biAb monovalently targeting CD19 and CD47 significantly reduced BCR-mediated B-cell proliferation to 10.5%, a level similar to the baseline level of 9.4% (Figure 1a).

The effect mediated by the biAb showed a trend of being more potent than the bivalent anti-CD19 mAb (88% vs 66% reduction, respectively, of BCR-mediated B-cell proliferation). The inhibitory effect of the CD19xCD47 biAb was not solely mediated by the anti-CD47 arm because antibody variants targeting CD47 monovalently or bivalently failed to abrogate cell proliferation triggered by BCR cross-linking (Figure 1a). Furthermore, combination of the anti-CD19 and anti-CD47 monovalent antibodies did not impair B-cell proliferation (Figure 1a). Together, these results highlighting the importance of the bispecificity with physical association (close proximity) of the anti-CD19 and anti-CD47 arms within a single molecule.

As FcγR-IIb (on B cells) is known to negatively affect B-cell proliferation, we also evaluated the contribution of this receptor to biAb-mediated inhibition of BCR-dependent B-cell proliferation.<sup>24</sup> The F(ab)<sub>2</sub> of the biAb, lacking the Fc-domain,

was equally effective as the full IgG to inhibit B-cell proliferation mediated by BCR cross-linking (Figure 1b), demonstrating that the biAb Fc domain was dispensable to the inhibitory activity of the biAb. Anti-CD19 mAbs were demonstrated to mediate B cell killing by direct cell death.<sup>25</sup> We therefore determined whether the inhibitory effect of the CD47xCD19 biAb and the anti-CD19 mAb on BCR-mediated B-cell proliferation observed here was attributable to induction of direct cell death. For this purpose, B cells were pretreated with the biAb or the bivalent anti-CD19 mAb before BCR-stimulation and B cell viability analyzed by flow cytometry. As shown in Figure 1c, in contrast to ibrutinib (a pro-apoptotic molecule), neither the biAb, nor the anti-CD19 mAb impaired primary B cell viability in the context of BCR stimulation.

### **Co-engaging CD47xCD19 inhibits BCR-induced cytokine production by human B cells**

B cells secrete several pro-inflammatory cytokines upon BCR stimulation.<sup>26</sup> We therefore evaluated whether co-ligating CD47xCD19 with a biAb or CD19 with the bivalent anti-CD19 mAb impaired BCR activation-mediated production of pro-inflammatory cytokines. After 5 days of culture with anti-BCR/anti-CD40 mAbs, analysis of cell supernatants from B cells isolated from 12 healthy donors showed an increased level of interleukin-6 (IL-6) and tumor necrosis factor (TNF) (Figure 2a and B, respectively). The burton tyrosine kinase (BTK) inhibitor, ibrutinib (used as a positive control to decrease cytokine production), inhibited BCR-mediated IL-6 and TNF production (Figure 2). Pretreatment with the CD47xCD19 biAb reduced the levels of IL-6 and TNF from 18.1 ± 9.7 pg/mL and 23.1 ± 9.6 pg/mL to 9.7 ± 6.9 pg/mL and 9 ± 3.9 pg/mL, respectively (Figure 2). Pretreating B cells with the anti-CD19 mAb before BCR stimulation also decreased both cytokine levels. Taken together, the results demonstrated that co-engaging CD47xCD19 with a biAb or targeting CD19 with a mAb significantly diminished anti-BCR/anti-CD40 mAbs-induced inflammatory cytokine secretion by human B cells.

### **CD47xCD19 co-engagement does not induce targeted receptor clustering or internalization**

To further investigate the mechanisms underlying the inhibition of B-cell proliferation induced by co-ligation of CD47 and CD19, the molecular events occurring at the B cell membrane were explored. Fluorescence resonance energy transfer (FRET) experiments were performed using a flow cytometry based method (FCET) to assess receptor clustering following antibody binding to cells. FCET revealed that both anti-CD20 (rituximab, used as a positive control of CD20 clustering upon bivalent engagement) and anti-CD19 bivalent antibodies (used to investigate homologous CD19 association) induced receptor clustering, with anti-CD20 and anti-CD19 mAbs increasing FCET values to 6.7 and 8.2 fold, respectively, compared to baseline levels (Figure 3a). The anti-CD19 monovalent antibody induced a significant level of FCET after 1 and 4 hours of incubation at 37°C (Figure 3a). Conversely, co-engaging CD47xCD19 with the biAb was unable to generate a FCET signal, highlighting the absence of CD19 clustering once co-engaged with CD47 at the surface

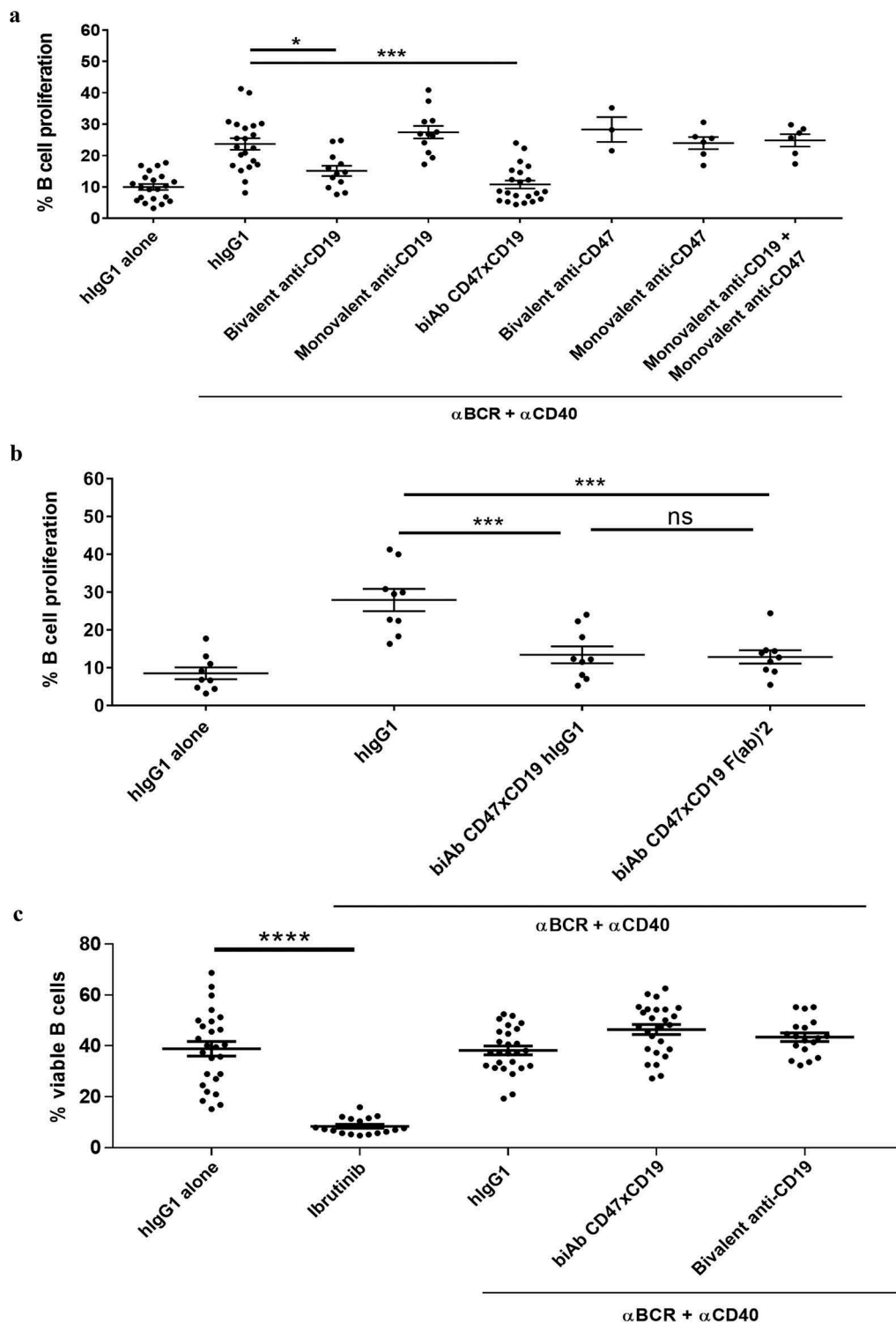


**Figure 1.** CD47/CD19 co-engagement inhibits B-cell proliferation triggered by BCR cross-linking.

**(a)** CFSE-labeled purified human primary B cells were incubated (15 min, RT) with either 10  $\mu$ g/mL of hlgG1 isotype control, bivalent or monovalent anti-CD19 antibodies, the CD47xCD19 biAb, bivalent or monovalent anti-CD47 antibodies or a combination of monovalent anti-CD19 and anti-CD47 antibodies. Cells were then stimulated with 5  $\mu$ g/mL anti-BCR (e.g. anti-IgM/IgG) and 1  $\mu$ g/mL anti-CD40 antibodies for 5 days at 37°C. As controls, B cells were incubated for 5 days with 10  $\mu$ g/mL hlgG1 isotype control in absence of BCR stimulation. **(b)** CFSE-labeled primary B cells were incubated (15 min, RT) with either 66.6 nM of hlgG1 isotype control, anti-CD47xCD19 biAb full-length IgG or F(ab)'2 before being stimulated with 5  $\mu$ g/mL anti-BCR and 1  $\mu$ g/mL anti-CD40 antibodies for 5 days. As controls, B cells were incubated for 5 days with 10  $\mu$ g/mL hlgG1 isotype control alone. **(c)** Human B cells were incubated with 10  $\mu$ g/mL hlgG1 isotype control or 10 nM ibrutinib (5 days, 37°C); or pretreated with 10  $\mu$ g/mL of hlgG1 control, anti-CD47xCD19 biAb or anti-CD19 mAb (15 min, RT) before being stimulated with 5  $\mu$ g/mL anti-BCR (e.g. anti-IgM/IgG) and 1  $\mu$ g/mL anti-CD40 antibodies (5 days, 37°C). Cells were then stained with a viability marker (BD Horizon 620) to detect live cells by flow cytometry. Graph represents the percentage of viable B cells. Each dot represents one unique donor as a source of B cells and the horizontal bars on each graph show the mean values  $\pm$  SEM. Statistical analysis was performed using the one way ANOVA test: \* $p < 0.05$ , \*\*\* $p < 0.001$ , ns = non-significant.

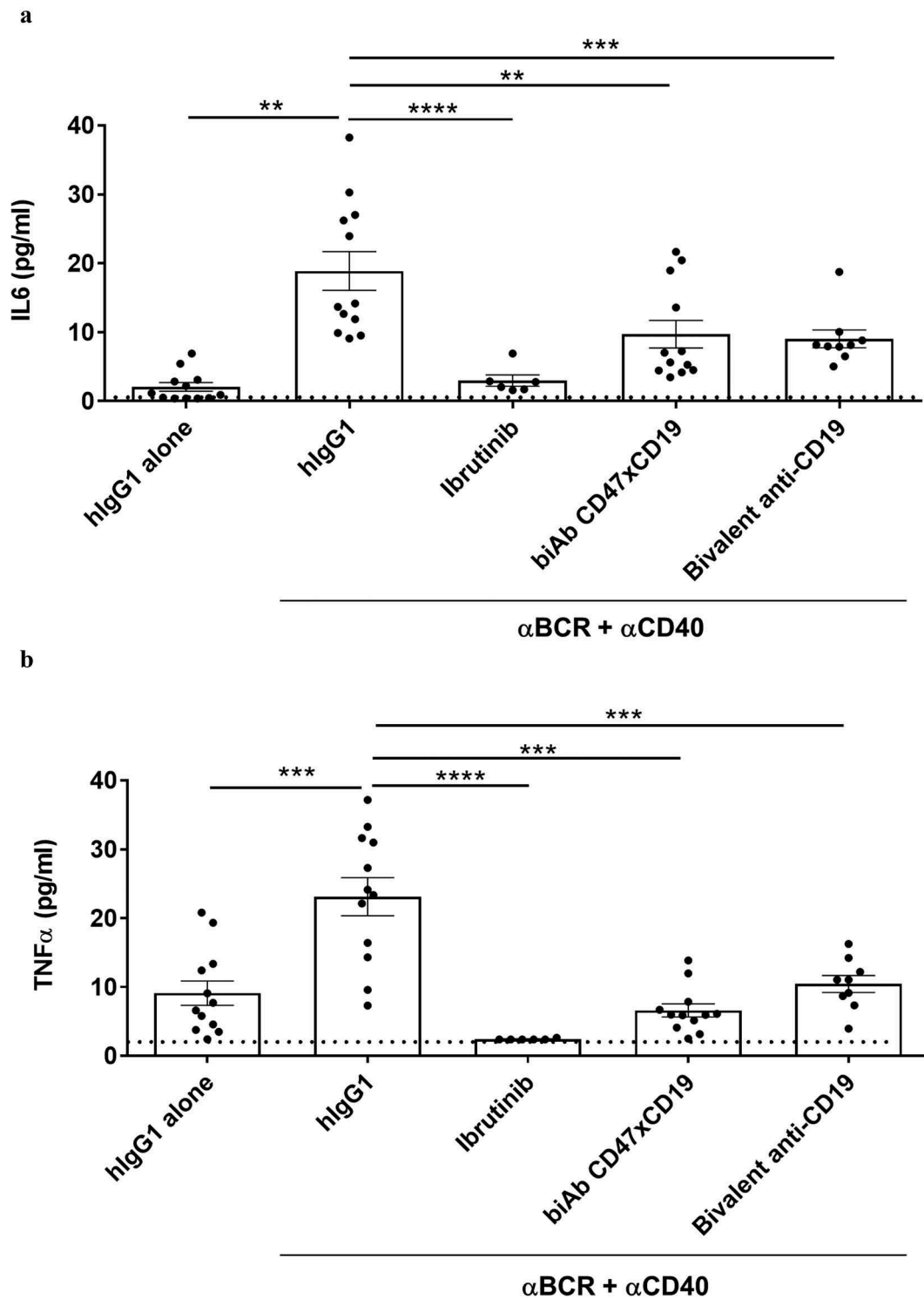


**Figure 2.** CD47/CD19 co-engagement inhibits BCR-induced cytokines production by human B cells.

Purified human B cells were pretreated with 10  $\mu\text{g}/\text{mL}$  hlgG1 isotype control, anti-CD47xCD19 biAb, bivalent anti-CD19 or 10 nM ibrutinib and then stimulated with 5  $\mu\text{g}/\text{mL}$  anti-BCR and 1  $\mu\text{g}/\text{mL}$  anti-CD40 antibodies. As controls, B cells pretreated with 10  $\mu\text{g}/\text{mL}$  hlgG1 isotype control were left unstimulated. After 5 days of incubation at 37°C, supernatants were harvested and IL-6 (**a**) and TNF (**b**) levels were measured by a multiplexing assay. Dashed lines represent the lower limit of cytokine detection. Data represent the mean values  $\pm$  SEM of a minimum of 6 independent donors. Statistical analysis was performed using the one way ANOVA test: \*\* $p < 0.01$ , \*\*\* $p < 0.001$ .

of B cells (Figure 3a). Analysis by confocal microscopy confirmed these observations as the anti-CD20 mAb induced punctuated staining, demonstrating the clustering of CD20 while, in contrast, the biAb did not, i.e., the labeling pattern remained homogenous (Figure 3b).

Next, the ability to induce target internalization was studied in order to assess whether this may have contributed to the impairment in BCR-mediated B-cell proliferation after ligating CD19, i.e., by lowering CD19 expression at the cell surface. Internalization kinetics of the fluorescent-labeled

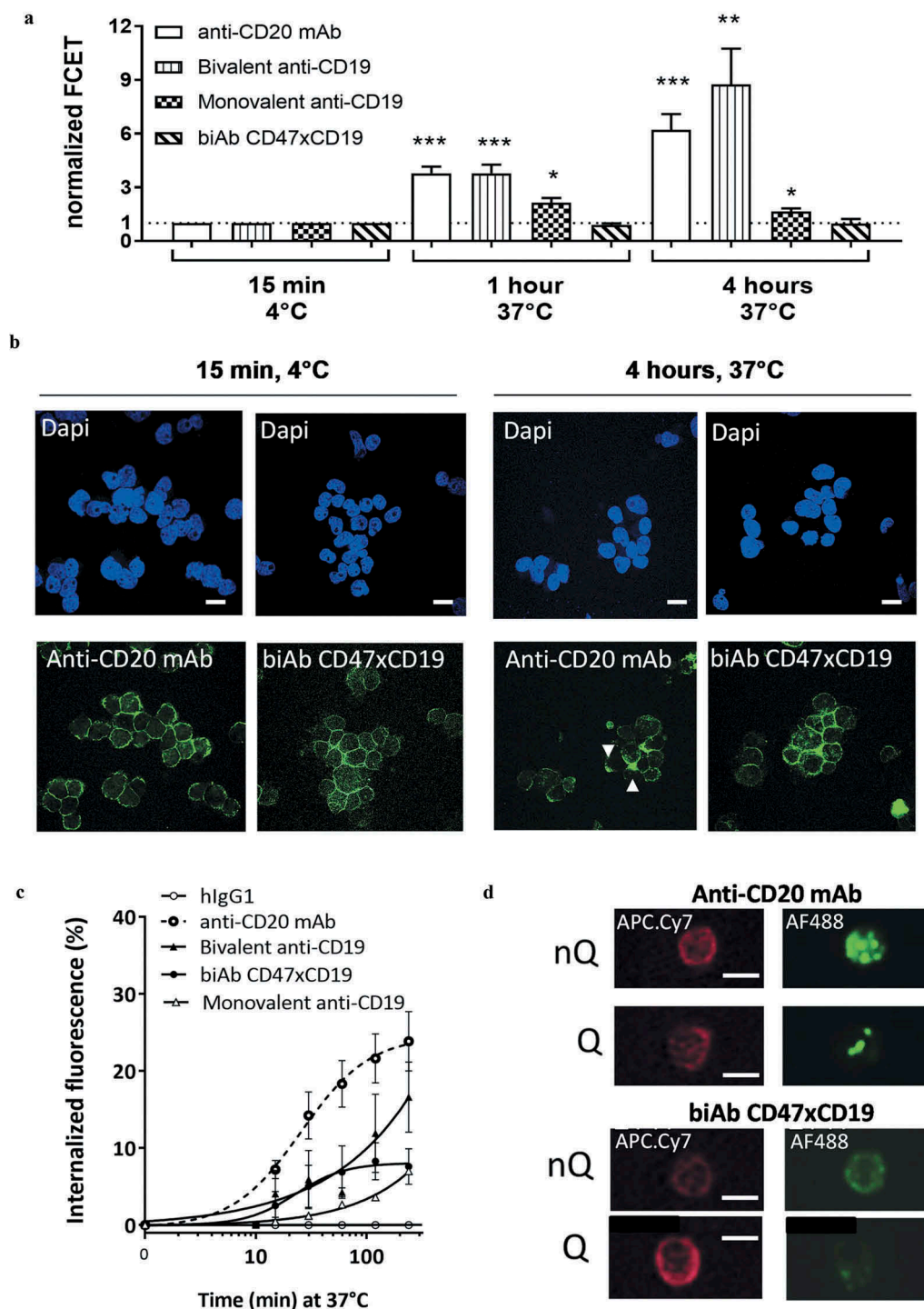


**Figure 3.** CD47/CD19 co-engagement does not induce receptor clustering or internalization.

(a) Targets clustering were quantified on living Raji B cells using a fluorescence resonance energy transfer applied in flow cytometry (FCET) approach. Anti-CD20 mAb, bivalent or monovalent anti-CD19 antibodies or anti-CD47xCD19 biAb were conjugated to the FRET pair Cy3/Cy5 (donor/acceptor molecules respectively), and energy transfer values were obtained by combining equimolar Cy3- and Cy5-labeled antibodies on Raji B cells after 1 to 4 hours at 37°C. The FRET value was calculated and presented as normalized FCET where the FCET values obtained for each pair Cy3/Cy5 antibodies incubated at 4°C were set at 1 defining a threshold (dashed line) above which a sample is considered positive for targets clustering. The average normalized FCET  $\pm$  SD were calculated from 3 independent experiments. (b) Images obtained by confocal microscopy of Raji B cells incubated with 10  $\mu$ g/mL Alexa Fluor 488 (AF488)-conjugated anti-CD20 mAb or anti-CD47xCD19 biAb for 15 min at 4°C or 4 hours at 37°C. The nuclei were counterstained with DAPI. Scale bars represent 10  $\mu$ m. The white arrows show anti-CD20 mAb clustering. (c) Raji B cells were incubated at 37°C with AF488-conjugated anti-CD20 mAb, anti-CD47xCD19 biAb or bivalent or monovalent anti-CD19 antibodies. Internalization fluorescence ((quenched fluorescence/unquenched fluorescence)  $\times$  100) was analyzed over time using flow cytometry. AF488-conjugated hlgG1 isotype control was used as a negative control to assess baseline internalization. The results are depicted as the mean internalized fluorescence  $\pm$  SEM of 4 independent experiments. The hlgG1 control is used as a negative control to assess baseline internalization. (d) Raji B cells were incubated (4 hours, 37°C) with AF488-conjugated anti-CD20 or anti-CD47xCD19 biAb then with an anti-CD45-APC.Cy7 to delimit B cell membrane. Cells were analyzed using a FlowSight instrument. AF488 fluorescence signals were captured without quenching (nQ) to assess total cell fluorescence and with quenching (Q) to visualize the fluorescence signal from the cytoplasmic compartment. Scale bars represent 10  $\mu$ m. Statistical analysis was performed using the one way ANOVA test: \* $p < 0.05$ , \*\* $p < 0.01$ , \*\*\* $p < 0.001$ .

biAb was assessed by measuring non-internalized (non-quenched, nQ) versus internalized (quenched, Q) fluorescence with time. The results demonstrated that targeting CD19 bivalently with the anti-CD19 mAb resulted in up to 20% receptor internalization after 4 hours of incubation at 37°C similarly to the positive control anti-CD20 mAb. In contrast, monovalent engagement of CD19 or co-engagement of CD47 and CD19 by the biAb resulted in lower, i.e., 7% internalization at 4 hours (Figure 3c). This level of internalization was confirmed by FlowSight imaging (Figure 3d). Thus, in contrast to an anti-CD19 mAb, bridging CD47 to CD19 with the biAb does not induce receptor clustering or internalization.

### **CD47xCD19 co-engagement prevents CD19 from migrating to BCR domains and impairs CD19-Y531 phosphorylation**

It has been demonstrated that CD19 regulates the threshold of BCR-mediated proliferation by associating with BCR clusters in lipid rafts to prolong BCR signaling.<sup>9,27</sup> Our results demonstrated that similar to an anti-CD19 or an anti-CD47 mAb, the CD47xCD19 biAb did not affect BCR clustering (supplementary Figure 2a) or intracellular Ca<sup>2+</sup> mobilization following BCR stimulation (supplementary Figure 2b). We next investigated whether CD47xCD19 co-ligation could impair CD19 and BCR association following BCR cross-linking using FCET. Incubation of the monovalent anti-CD19 antibody with an anti-BCR mAb induced the direct association over time of CD19 with the BCR (Figure 4a), recording a FCET value of 2.6 units at 30 minutes (min) and 3.6 units at 1 hour of BCR stimulation. Pre-incubation with the anti-CD19 mAb did not significantly affect the clustering between CD19 and BCR at 30 min or 1 hour. In contrast to the anti-CD19 mAb, co-engaging CD47xCD19 with the biAb significantly impaired receptor association to the BCR with a FCET value of 1.5 units at 30 min and of 1.9 units at 1 hour of BCR stimulation (Figure 4a).

CD19 is rapidly phosphorylated upon BCR stimulation.<sup>12,14</sup> To address whether this impaired CD19/BCR association affected CD19 phosphorylation, we assessed CD19 phosphorylation at tyrosine(Y)-531, which contributes to the transduction of CD19 signaling.<sup>14</sup> As expected, pretreatment of malignant B cells with human IgG1 isotype control and incubation with an anti-BCR mAb resulted in substantial CD19-Y531 phosphorylation at 1 min of incubation (Figure 4a and c). The signal decreased at 5 min and returned to baseline level at 15 min. In contrast to a monovalent engagement of CD19, pretreatment with the anti-CD47xCD19 biAb resulted in a significant decrease in CD19-Y531 phosphorylation (Figure 4b and 4c). The same samples were tested for phosphorylation of Syk (BCR-specific tyrosine kinase) and MAPK (common tyrosine kinase to BCR and CD19 signaling). BCR cross-linking induced both Syk-Y352 and MAPK phosphorylation, which were unaffected by any of the pretreatment tested, including the CD47xCD19 biAb (Figure 4b). Together, these results indicate that the anti-CD47xCD19 biAb did not impede BCR clustering, but decreased CD19 association to the BCR, leading to decreased CD19 phosphorylation upon BCR activation.

### **CD47xCD19 co-engagement alters a subset of BCR-induced genes distinct from those affected by the anti-CD19 mAb**

To further elucidate the inhibitory mechanism of CD47xCD19 co-engagement on BCR-mediated B-cell proliferation, RNA sequencing was performed to identify potential gene modifications. Of the 35,000 genes tested, stimulation by BCR cross-linking altered the expression of 5,473 genes, with the majority linked to cell metabolism (3,072 genes), cell communication (1,291 genes), protein transport (794 genes), cell death (743 genes) and intracellular signaling (727 genes) (Figure 5a). We observed that among the 5473 genes altered by BCR cross-linking, 29 genes were significantly affected by CD47xCD19 co-ligation and 24 genes showed significant changes in response to the pretreatment with anti-CD19 mAb (Supplementary Figures 3 and 4). Among the set of genes affected by CD47xCD19 co-ligation and the set of genes affected by anti-CD19 mAb, only two genes were common to both sets (ARHGEF11 and ASCL2) (Supplementary Figures 3 and 4). The biAb-affected genes with known functions were clustered to biological processes, including cell signaling (AMER2 and FES), remodeling of the cytoskeleton (DNAH8, TP63, ARHGEF4, ARHGEF11 and POF1B), inflammation (NLRP12 and IL10) and metabolism (MGAT3) (Figure 5b and c). The largest cluster of genes significantly affected by CD47xCD19 co-engagement were those involved in cytoskeleton remodeling, including 4 genes (DNAH8, TP63, POF1B and ARHGEF4) that were significantly decreased, and one gene (ARHGEF11) that was significantly increased (Figure 5c). The largest cluster of genes significantly affected by the anti-CD19 mAb included those involved in apoptosis/cell cycle processes (4 genes in total: LCN2, TEAD4, POLQ and RASSF6) (Figure 5d). Several genes involved in other biological processes, such as the actin-binding partner GRID2IP in cytoskeleton remodeling, ESR1 and GPRC5B in cell signaling and SDS in metabolism, were also only significantly affected by CD19 mAb treatment but not by CD47xCD19 biAb (Figure 5d). These results suggest that co-engaging CD47xCD19 on B cells can modulate a pattern of BCR-induced genes involved in multiple biological processes different from the genes significantly impacted by cross-linking CD19 with an anti-CD19 mAb.

## **Discussion**

Small molecules inhibiting BCR signaling and B-cell depletion therapy using anti-CD20 antibodies represent a major therapeutic advance in B cell malignancies as well as autoimmune diseases. However, both therapeutic strategies have limitations, and the clinical responses to these therapies are heterogeneous among patients.<sup>28,29</sup> The BCR-inhibiting molecules are only efficacious when BCR signaling is pivotal to disease progression, but not expected to have any effect on BCR-independent B-cell proliferation. The CD47xCD19 biAb presented herein is therefore expected to be efficacious in both BCR-dependent and BCR-independent diseases since, in addition to inhibiting BCR-dependent B-cell proliferation, the biAb can also deplete abnormal B cells through BCR-independent, Fc-mediated effector functions.<sup>23</sup> B-cell depletion using anti-CD20 antibodies is dependent on CD20 expression on target cells and a micro-environment in disease tissues favoring

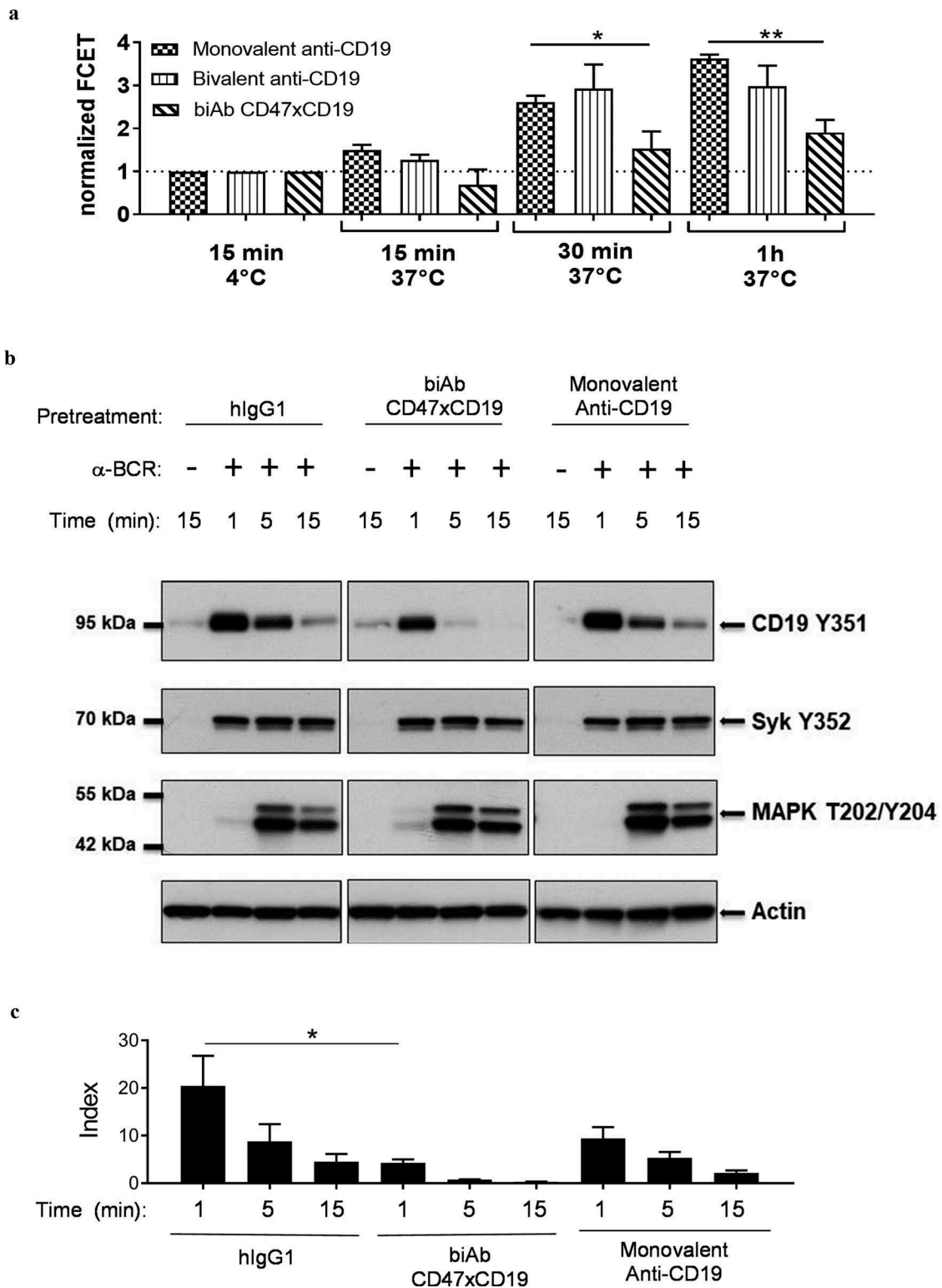


**Figure 4.** CD47/CD19 co-engagement interferes with CD19 migration to the BCR and impairs CD19 phosphorylation upon BCR cross-linking.

**(a)** Ramos B cells were incubated with equimolar amount of Cy3-labeled anti-BCR (e.g., anti-IgM) and Cy5-labeled monovalent or bivalent anti-CD19 or anti-CD47xCD19 biAb (15 min, 30 min or 1 hour, 37°C) before being washed and analyzed for FRET by flow cytometry. Data are presented as normalized FCET where the FCET values obtained for each Cy3/Cy5 pair of antibodies incubated at 4°C were set at 1 defining a threshold (dashed line) above which a sample is considered positive for targets clustering. Graph represents the mean  $\pm$  SEM from three independent experiments. **(b, c)** Ramos B cells were serum-starved for 5 hours and pretreated with 10  $\mu$ g/mL of hlgG1 isotype control, anti-CD47xCD19 biAb or monovalent anti-CD19 (15 min, RT) before activation by BCR-crosslinking with an anti-IgM for the indicated time points at 37°C. Cell lysates were fractionated by SDS-PAGE and transferred onto nitrocellulose for subsequent immunoblotting to assess phosphorylation of CD19-Y531, Syk-Y352 and MAPK (Erk1/Erk2)-T202/Y204. Actin is used as a control of protein loading. **(b)** One representative western blot experiment from three independent ones is shown. **(c)** The ratio of phospho-CD19-Y531 over actin signal intensities were calculated and converted to index relative to unstimulated B cells. Data show mean index  $\pm$  SEM of three independent experiments. Statistical analysis was performed using the one way ANOVA test: \* $p < 0.05$ .

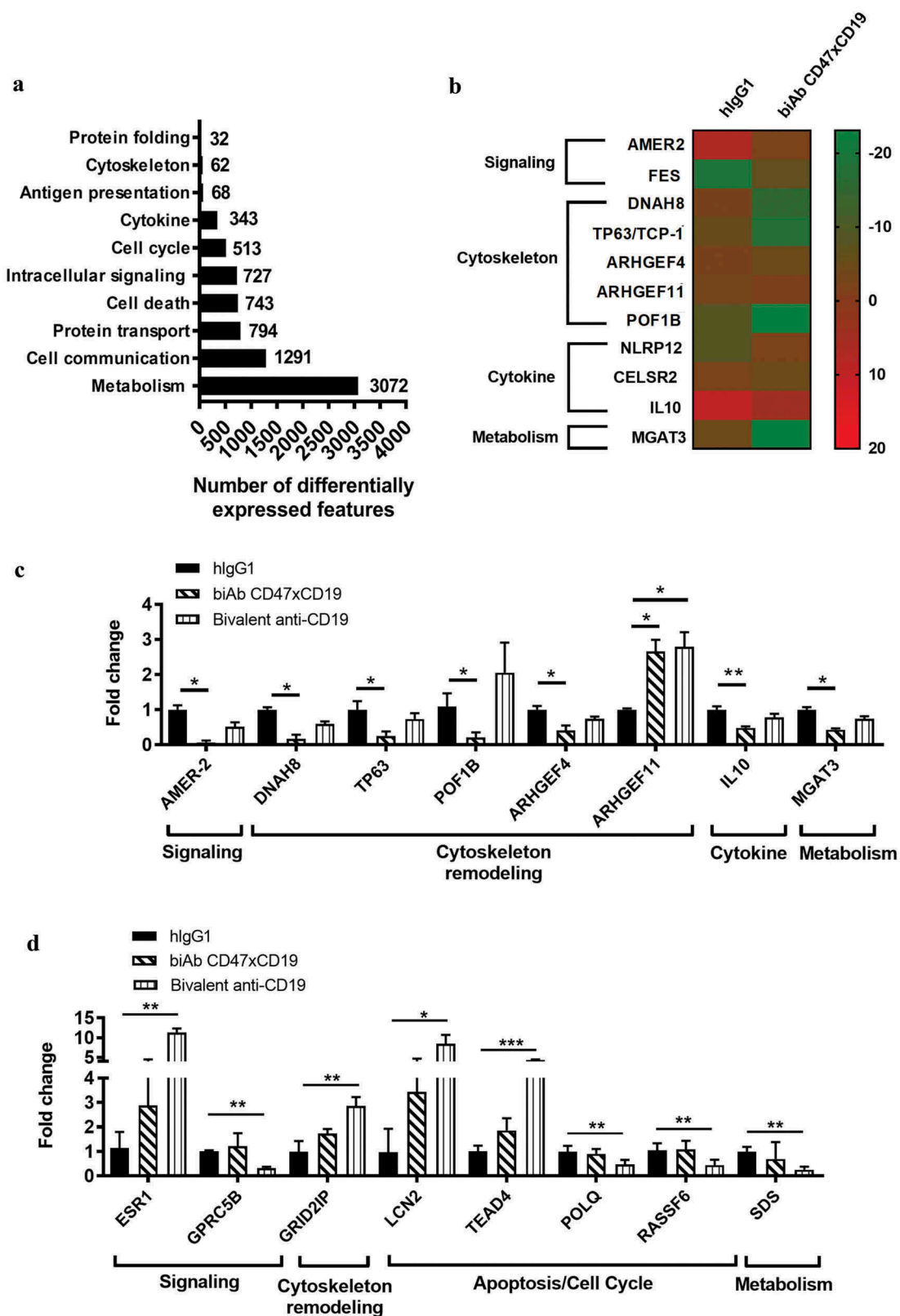


**Figure 5.** BCR-induced gene expression changes in response to CD47xCD19 co-engagement.

Purified human primary B cells were pretreated (15 min, RT) with 10  $\mu\text{g}/\text{mL}$  hlgG1 isotype control, anti-CD47xCD19 biAb or bivalent anti-CD19 and then stimulated with 5  $\mu\text{g}/\text{mL}$  anti-BCR and 1  $\mu\text{g}/\text{mL}$  anti-CD40 antibodies. After incubation (4 hours, 37°C), total RNA were isolated for subsequent investigation by RNA sequencing. **(a)** Number of differentially expressed features and their functional classification identified in response to BCR stimulation. **(b)** Heatmap of the genes differentially expressed between the hlgG1-treated group and anti-CD47xCD19 biAb-treated group. The color key represents fold of induction of each gene over the unstimulated control. Genes are classified according to their biological function. **(c)** Relative expression levels of the genes differentially expressed between the hlgG1-treated group and the anti-CD47xCD19 biAb-treated group or **(d)** the bivalent anti-CD19 mAb-treated group. The values were normalized to the mean expression level in the hlgG1-treated group, which was arbitrarily set as 1. Data shown are the mean values  $\pm$  SEM of each gene from three B cell donors. Statistical analysis was performed using the paired T test: \* $p < 0.05$ , \*\* $p < 0.01$ , \*\*\* $p < 0.05$ .



Fc-mediated effector functions including complement-dependent cytotoxicity, antibody-dependent cell-mediated cytotoxicity or antibody-dependent cellular phagocytosis (ADCP).<sup>30</sup> Malignant B cells may escape anti-CD20 therapies by either down-regulating CD20 expression or modulating the tumor microenvironment to suppress Fc-mediated effector functions (e.g., upregulating CD47 expression to suppress macrophage-mediated ADCP or reducing immune cell infiltration).<sup>31–33</sup> By targeting another B-cell-specific antigen, i.e., CD19, and blocking CD47/SIRP $\alpha$  interaction (i.e., enhancing macrophage-mediated ADCP), the CD47xCD19 biAb is well-positioned to address these two major mechanisms underlying the resistance/relapse to anti-CD20 therapies. Furthermore, by having an Fc-independent mechanism of inhibiting B-cell proliferation, the biAb may be efficacious even in tumor regions poorly infiltrated by Fc $\gamma$ R-positive effector cells. Further investigation would be required, although out of the scope of the current study, to confirm whether the reported segregation of CD19 from BCR domains in preventing BCR-mediated B-cell proliferation would be also observed in *in vivo* settings.

To dissect the mechanism by which the CD47xCD19 biAb influences BCR-mediated B-cell proliferation, the effect was compared to antibodies engaging monovalently CD19 or CD47 or the combination of both variants. These controls had no effect on B-cell proliferation, suggesting that co-ligating CD19 to CD47 with the CD47xCD19 biAb is required. Increasing the concentration of monovalent anti-CD19 antibody to saturate CD19 target did not show any effect on B-cell proliferation either. Due to the low affinity of the anti-CD47 monovalent antibody (no apparent binding to human B cell at the highest concentration testable *in vitro*), it is impossible to have a combination condition mimicking the same levels of binding to both cell surface CD47 and CD19 as with the biAb condition. Furthermore, the inhibitory effect is independent of the inhibitory Fc $\gamma$ R-IIB, in contrast to antibodies targeting CD19, where the inhibitory Fc $\gamma$ R-IIB has been recently demonstrated to inhibit B-cell proliferation and cytokine production in response to BCR crosslinking.<sup>34</sup> Interestingly, treatment with the CD19 mAb enhanced CD19 clustering, a prerequisite for antibody-target complex internalization,<sup>35</sup> while CD19 clustering was not detected in the presence of the CD47xCD19 biAb, an observation confirmed by the experiment evaluating receptor internalization. Thus, removing a limited pool of CD19 from B cell surface did not contribute to the inhibition of B-cell proliferation afforded by the biAb.

Recent advances in live-cell imaging technologies have demonstrated the importance of BCR/CD19 co-clustering in the initiation of BCR signaling.<sup>9,36</sup> Our data demonstrate that, in contrast to a bivalent engagement of CD19, the CD47xCD19 biAb prevent the recruitment of CD19 to the BCR activating cluster upon BCR cross-linking. It is worth noting that, on erythrocytes, it has been shown that CD47 is anchored to the cytoskeleton hindering CD47 mobility on the membrane.<sup>37,38</sup> Coupling this reported observation with our data on the ability for the CD47xCD19 biAb to sequester CD19 from BCR clusters, co-ligation of CD19 and CD47 by the biAb may indeed restrict the CD19 mobility at the B cell surface by the cytoskeleton-anchored glycoprotein CD47. This effect would prevent CD19 from being mobilized to the BCR

signaling complex, highlighting an unexpected role of CD47 co-ligation with CD19 in inhibiting B-cell proliferation.

Recent studies demonstrate that antigen-driven BCR clusters are efficiently converted to a signaling active state by co-localization with CD19 clusters.<sup>9,36,39</sup> As such, we investigated the impact of bridging CD47xCD19 on early BCR signaling events. The CD47xCD19 biAb did not impair the level of intracellular calcium mobilization or Syk and MAPK-phosphorylation following BCR stimulation. Instead, treatment with the biAb resulted in decreased CD19 Tyr531 phosphorylation upon BCR stimulation.

The differences observed following CD47xCD19 biAb versus CD19 mAb ligation on BCR/CD19 clustering are further reflected by their differential modulation of gene expression following BCR cross-linking. The CD47xCD19 co-engagement induced significant changes in a unique set of genes involved in several biological processes, including signaling, metabolism and cytoskeleton remodeling. The largest subset of genes affected by the CD47xCD19 biAb are related to the cytoskeleton remodeling by decreasing the level of actin binding proteins (e.g., POF1B), the dynein heavy chain (e.g., DNAH8) or the Rho GTP exchange factor ARHGEF4 described to regulate actin and microtubule cytoskeleton networks.<sup>40–43</sup> In contrast, the anti-CD19 mAb altered a set of BCR-inducible genes linked to apoptosis/cell cycle biology. This is in line with a previous report demonstrating that anti-CD19 bivalent engagement impacts the B cell cycle.<sup>44</sup> These data further support that the biAb and the anti-CD19 mAb employ distinct mechanisms to tune BCR-induced gene expression. The role of cytoskeleton remodeling in BCR-stimulated B cell activation has been well-established. In response to membrane antigen ligation, B cells respond with an initial spreading (e.g., B cell membrane protrusion to sense local microenvironment) to better collect antigens, which is followed by the clustering of BCRs at the immune synapse.<sup>45</sup> Both the initial spreading and the consequent clustering of BCRs require reorganization of the cytoskeleton network.<sup>46–48</sup> Thus, the binding of the CD47xCD19 biAb may inhibit B cell activation at least partially by modulating genes involved in cytoskeleton dynamics.

Taken together, this study demonstrates that co-ligation of CD47xCD19 with a biAb, in addition to mediating killing of tumor B cells by macrophage-mediated phagocytosis, can alter the dynamics of CD19 mobility at the plasma membrane, phosphorylation of CD19 and BCR-mediated gene expression.<sup>23</sup> These mechanisms could be exploited to dampen the response of BCR-activated B cells in settings of malignancies and autoimmunity.

## Materials and methods

### Reagents

CD47xCD19 biAb, Ab variants engaging monovalently CD47 or CD19, bivalent anti-CD47 or CD19 mAbs were generated and purified at NovImmune as described in details by Fischer et al.<sup>49</sup> The anti-CD47 monovalent antibody used in this study contains the same CD47-binding arm as the CD47xCD19 biAb and an arm binding to an irrelevant target (EpCam, a target not expressed in human B cells). The anti-CD19 monovalent antibody contains the

same CD19-binding arm as the CD47xCD19 biAb and an irrelevant nonbinding arm (with no detectable binding to any known human protein). Human IgG1 (hIgG1) isotype control mAb was generated internally from Chinese Hamster Ovary (CHO) culture supernatant. The CD19 monovalent antibody contains the same anti-CD19 arm as the CD47xCD19 biAb and an irrelevant non-binding arm. In the same manner, the CD47 monovalent variant contains the same CD47 arm as the biAb and an irrelevant nonbinding arm. Clinical grade rituximab (anti-CD20 hIgG1 mAb) was obtained from FarmaMondo. F(ab)<sup>2</sup> goat anti-human IgM/IgG antibodies (109–006-127) were purchased from Jackson ImmunoResearch and anti-CD40 antibody (Clone 82111, MAB6321) from R&D Systems. Phospho-CD19 (Y531, 3571), phospho-Syk (Y352, 2701), and phospho-MAPK (T202/Y204, 9101) were purchased from Cell Signalling Technology. Anti-actin Ab was purchased from Sigma (A1978) and horseradish peroxidase (HRP)-conjugated goat anti-rabbit (111–036-003) or anti-mouse IgG (115–036-003) were purchased from Jackson ImmunoResearch.

### **Isolation of human primary B cells**

Peripheral blood mononuclear cells were isolated by density gradient centrifugation on SepMate-Ficoll tubes (StemCell Technologies, 85,450) and B cells were purified by negative selection using Magnetic Bead-Activated Cell Sorting (StemCell Technologies, 17,954) according to the manufacturer's protocol. B cell purity (>95%) was assessed by flow cytometry using anti-human CD20-APC (BD Biosciences, 559,776).

### **BCR activation and proliferation assay**

Isolated B cells were incubated with 0.2  $\mu$ M carboxylfluorescein diacetate succinimidyl ester (CFSE, ThermoFisher Scientific, C34554) in phosphate-buffered saline (PBS) for 15 min at 37°C, washed several times with complete RPMI medium (containing 10% calf serum, 2mM L-glutamine, 1mM sodium pyruvate, 10mM HEPES, 50 $\mu$ M 2-mercaptoethanol and 25 $\mu$ g/mL gentamicin) and transferred into 96-well plates (0.5x10<sup>5</sup> cells/well). B cells were pretreated with 10  $\mu$ g/mL of hIgG1, anti-CD47, anti-CD19 mAbs, CD47xCD19 biAb or the variants antibody engaging monovalently either CD47 or CD19 (alone or in combination tested at 10  $\mu$ g/mL each) (15 min, room temperature). In some conditions, the F(ab)<sup>2</sup> fraction of the CD47xCD19 biAb was generated using the FragIT kit (Genovis, AO-FR6-025) and used at 66.6 nM to have the same molar quantity of antibodies per condition. Cells were then stimulated by cross-linking of the BCR with 5  $\mu$ g/mL of anti-human IgM/IgG F(ab)<sup>2</sup> in the presence of 1  $\mu$ g/mL of anti-CD40 antibodies (combination referred as BCR-stimulation) and incubated in complete medium (5 days, 37°C). Cells were then stained with BD Horizon 620 (BD Biosciences, 564,996) to exclude dead cells. CFSE staining was analyzed on live cells by flow cytometry using a CytoFLEX (Beckman Coulter) and results evaluated by FlowJo software.

### **Cytokine production**

Isolated B cells were pre-treated and stimulated as described above. The supernatants were collected after 5 days and stored

at –70°C until analyzed for the presence of IL-6 and TNF by a multiplexing assay (Luminex 200 System, xPONENT 3.1 software).

### **Fluorescence resonance energy transfer applied in flow cytometry assay**

Antibodies were conjugated to NHS-ester derivatives of Cy3 and Cy5 (Novus Biologicals, 340–0010) as described in the manufacturer's instruction. FCET methodology was applied as previously described.<sup>50</sup> An energy transfer between the Cy3-labeled and the Cy5-labelled antibody measured by FCET indicate that the two antibody molecules bind to targets in close proximity, thus indicating receptor clustering. Raji or Ramos B cells were resuspended in PBS and distributed in 96-well plates (1x10<sup>5</sup> cells/well). Equimolar donor (Cy3)-conjugated and acceptor (Cy5)-conjugated antibodies were combined and added to the cell suspension (20  $\mu$ g/mL final). Cells were incubated from 15 min to 4 hours in the dark at 37°C or 15 min on ice. B cells were co-incubated with both the Cy3-labeled test antibody and the same antibody labeled with Cy5. Alternatively, to address BCR and CD19 clustering, B cells were incubated with combined Cy3-labeled anti-BCR (i.e., anti-IgM) and Cy5-labeled test antibodies. Each experiment included cells labeled with donor or acceptor-conjugated antibodies in the presence of equimolar unlabeled antibodies. FCET was assessed on living B cells using flow cytometry (CytoFLEX, Beckman Coulter). By subtracting values collected from single-labeled cells and respective isotype controls, a high FCET value indicated close proximity of Cy3- and Cy5-labeled antibodies.

### **Internalization assay**

Fluorescent labelled-antibodies were generated using an AF488 labeling kit (Life Technologies, A-20,181) according to manufacturer's instructions. Raji B cells were pre-incubated (30 min, 4°C) with 50  $\mu$ g/mL AF488-conjugated CD47xCD19 biAb or control antibodies, a concentration at which surface staining was determined to be saturating. Cells were then incubated (from 15 min to 4 hours, 37°C) in complete culture medium. After incubation, cells were rapidly chilled on ice, washed in cold PBS and incubated (30 min, 4°C) with (quenched samples) or without (unquenched samples) a saturating concentration (100  $\mu$ g/mL) of rabbit anti-AF 488 quenching polyclonal antibodies (Life Technologies, A-11094). Cells were fixed in CellFix (BD Biosciences, 340181) before acquisition on a flow cytometer and data were generated using FlowJo software. Internalized fluorescence was then calculated from data of quenched and unquenched samples by correcting for incomplete surface quenching. In some experiments, internalization was confirmed using a second technology, the FlowSight imaging flow cytometer (Merck Millipore).

### **Western blot analysis**

Ramos B cells were first starved during 5 hours in serum-free RPMI. Then, cells (0.25x10<sup>6</sup> per tube in 50  $\mu$ L) were either left untreated or pretreated 15 min at room temperature (RT) with 10  $\mu$ g/mL anti-CD47xCD19 biAb, monovalent anti-CD

19 or hIgG1 isotype control. Cells were then stimulated with an anti-IgM (10 µg/mL) for 1, 5 and 15 min at 37°C, pelleted and lysed in 35 µl of Laemmli buffer (BioRad, 161-0747) containing 0.1M dithiothreitol. Cell lysates were boiled 5 min at 95°C before being subjected to 10% sodium dodecyl sulfate-polyacrylamide gel electrophoresis (SDS-PAGE) and proteins were transferred to nitrocellulose membranes (GE Healthcare Life Sciences). Membranes were blocked for 30 min in Tris-buffered saline-Tween (TBS-T, 150 mM NaCl, 20 mM Tris and 0.1% Tween 20, pH 7.5) containing 5% milk and incubated overnight at 4°C with primary antibodies diluted in TBS-T 1% milk. After three washes in TBS-T, HRP-conjugated secondary antibodies diluted in TBS-T 1% milk were added for 1 hour at RT. After three washes in TBS-T, reactive proteins were visualized using an enhanced chemiluminescence detection system (Millipore). Phospho-CD19 signal intensities were quantified using Image J and corrected for protein loading by the use of Actin. Results were presented as index values relative to unstimulated conditions.

### RNA sequencing analysis

Human primary B cells (0.15x10<sup>6</sup> cells/mL) were pretreated with 10 µg/mL of hIgG1, anti-CD19 mAb, anti-CD47xCD19 biAb (15 min, RT) or left untreated as control (unstimulated B cells). Cells were then stimulated by cross-linking of the BCR with 5 µg/mL of anti-human IgM/IgG F(ab)<sup>2</sup> in the presence of 1 µg/mL of anti-CD40 antibodies and incubated in complete medium (4 hours, 37°C). Total RNA were isolated using the reliaPrep RNA cell Miniprep System (Promega, Z6011), DNA contaminant was removed using the DNA removal kit (ThermoFisher Scientific, AM1906) and RNA quality was verified using the Agilent 2100 bioanalyzer. RNA samples were then collected to prepare a library for sequencing on an Illumina HiSeq 4000. Biological triplicate samples were sequenced at the iGE3 Genomics Platform of the University of Geneva. The reads were mapped to the reference genome (UCSB – hg38) and the differential expression investigated (softwares TopHat v2.0.13 and R/Bioconductor EdgeR v3.10.5., respectively). BCR-induced genes with at least 2-fold change in expression and with an adjusted p value ≤ 0.05 in response to each pretreatment were chosen for further analysis. Functional classification of genes was performed using MetaCore (Life Sciences Research, Thomson Reuters).

### Statistical analysis

GraphPad Prism 6 was used for all statistical analysis. The one-way ANOVA was used for comparing difference between groups \*\*\* p < 0.001, \*\* p < 0.01, \* p < 0.05. Data are presented as mean ± SEM.

### Abbreviations

ADCP	Antibody-Dependent Cellular Phagocytosis
AF488	Alexa-Fluor 488
AKT	Protein kinase B
APC	Allophycocyanin
biAb	Bispecific antibody
BCR	B Cell Receptor

BTK	Burton Tyrosine Kinase
CAR-T	Chimeric Antigen Receptor T
CD	Cluster of Differentiation
CFSE	Carboxyfluorescein
CHO	Chinese Hamster Ovary
CLL	Chronic Lymphocytic Leukemia
Cy	Cyanine
DAPI	4',6-Diamidino-2-Phenylindole
DNA	Deoxyribonucleic Acid
FRET	Fluorescence Resonance Energy Transfer
FCET	Fluorescence resonance Energy Transfer using Flow cytometry
Fc	Fragment Crystallizable
FcγR	Fc gamma Receptor
HEPES	4-(2-Hydroxyethyl)Piperazine-1-EthaneSulfonic acid
HRP	Horseradish Peroxidase
IgG	Gamma Immunoglobulin
IL-6	InterLeukin-6
mAb	monoclonal antibody
MAPK	Mitogen-Activated Protein kinase
min	minutes
NHS	N-Hydroxysuccinimide
nQ	non-quenched fluorescence
PBS	Phosphate-Buffered Saline
PI3K	phosphoinositide-3 kinase
Q	quenched fluorescence
RPMI	Roswell Park Memorial Institute
RNA	Ribonucleic Acid
RT	Room Temperature
SD	Standard Deviation
SDS-PAGE	Sodium Dodecyl Sulfate Polyacrylamide Gel Electrophoresis
SIRP-α	Signal Regulatory Protein alpha
Syk	Spleen Tyrosine Kinase
TBS-T	Tris-Buffered Saline-Tween
TNFα	Tumor Necrosis Factor alpha
Y	tyrosine

### Acknowledgments

E.H., L.B., N.N., B.D.W., M.K.V. W.F., L.S., and V.B., were involved in designing the study plan. E.H., L.B., N.N., B.D., J.P.A.L., F.R., B.D.W., were involved in data collection and interpretation of data. E.H., L.B., N, N, M.K.V. W.F., L.S., and V.B., were involved in interpretation of data and revising the manuscript. We thank Ana-Maria Lennon-Duménil (Institut Curie, Paris) for helpful discussions and comments.

### Disclosure of Potential Conflicts of Interest

E.H., L.B., B.D., F.R., M.K.V., W.F., L.S. and V.B. are employees of Novimmune SA, whose CD47xCD19 biAb antibody was used in this study. The other authors declare no conflict of interests.

### ORCID

Nelly Noraz  <http://orcid.org/0000-0003-4076-9773>  
 Jean-Pierre Aubry-Lachainaye  <http://orcid.org/0000-0002-7785-1191>  
 Walter Ferlin  <http://orcid.org/0000-0001-5636-4450>

### References

1. Kraus M, Alimzhanov MB, Rajewsky N, Rajewsky K. Survival of resting mature B lymphocytes depends on BCR signaling via the Igalphabeta heterodimer. *Cell*. 2004;117:787–800. doi:10.1016/j.cell.2004.05.014.
2. Monroe JG. Ligand-independent tonic signaling in B-cell receptor function. *Curr Opin Immunol*. 2004;16:288–295. doi:10.1016/j.coi.2004.03.010.

3. Monroe JG. ITAM-mediated tonic signalling through pre-BCR and BCR complexes. *Nat Rev Immunol.* 2006;6:283–294. doi:10.1038/nri1808.
4. Young RM, Wu T, Schmitz R, Dawood M, Xiao W, Phelan JD, Xu W, Menard L, Meffre E, Chan WC, et al. Survival of human lymphoma cells requires B-cell receptor engagement by self-antigens. *Proc Natl Acad Sci U S A.* 2015;112:13447–13454. doi:10.1073/pnas.1514944112.
5. Corso J, Pan KT, Walter R, Doebele C, Mohr S, Bohnenberger H, Strobel P, Lenz C, Slabicki M, Hullein J, et al. Elucidation of tonic and activated B-cell receptor signaling in Burkitt's lymphoma provides insights into regulation of cell survival. *Proc Natl Acad Sci U S A.* 2016;113:5688–5693. doi:10.1073/pnas.1601053113.
6. Niemann CU, Wiestner A. B-cell receptor signaling as a driver of lymphoma development and evolution. *Semin Cancer Biol.* 2013;23:410–421. doi:10.1016/j.semcancer.2013.09.001.
7. Fearon DT, Carroll MC. Regulation of B lymphocyte responses to foreign and self-antigens by the CD19/CD21 complex. *Annu Rev Immunol.* 2000;18:393–422. doi:10.1146/annurev.immunol.18.1.393.
8. Buhl AM, Pleiman CM, Rickert RC, Cambier JC. Qualitative regulation of B cell antigen receptor signaling by CD19: selective requirement for PI3-kinase activation, inositol-1,4,5-trisphosphate production and Ca<sup>2+</sup> mobilization. *J Exp Med.* 1997;186:1897–1910. doi:10.1084/jem.186.11.1897.
9. Depoil D, Fleire S, Treanor BL, Weber M, Harwood NE, Marchbank KL, Tybulewicz VL, Batista FD. CD19 is essential for B cell activation by promoting B cell receptor-antigen micro-cluster formation in response to membrane-bound ligand. *Nat Immunol.* 2008;9:63–72. doi:10.1038/ni1547.
10. Otero DC, Rickert RC. CD19 function in early and late B cell development. II. CD19 facilitates the pro-B/pre-B transition. *J Immunol.* 2003;171:5921–5930. doi:10.4049/jimmunol.171.11.5921.
11. Otero DC, Anzelon AN, Rickert RC. CD19 function in early and late B cell development: I. Maintenance of follicular and marginal zone B cells requires CD19-dependent survival signals. *J Immunol.* 2003;170:73–83. doi:10.4049/jimmunol.170.1.73.
12. Ishiura N, Nakashima H, Watanabe R, Kuwano Y, Adachi T, Takahashi Y, Tsubata T, Okochi H, Tamaki K, Tedder TF, et al. Differential phosphorylation of functional tyrosines in CD19 modulates B-lymphocyte activation. *Eur J Immunol.* 2010;40:1192–1204. doi:10.1002/eji.200939848.
13. Otero DC, Omori SA, Rickert RC. Cd19-dependent activation of Akt kinase in B-lymphocytes. *J Biol Chem.* 2001;276:1474–1478. doi:10.1074/jbc.M003918200.
14. Wang Y, Brooks SR, Li X, Anzelon AN, Rickert RC, Carter RH. The physiologic role of CD19 cytoplasmic tyrosines. *Immunity.* 2002;17:501–514.
15. Engel P, Zhou LJ, Ord DC, Sato S, Koller B, Tedder TF. Abnormal B lymphocyte development, activation, and differentiation in mice that lack or overexpress the CD19 signal transduction molecule. *Immunity.* 1995;3:39–50.
16. Sato S, Steeber DA, Tedder TF. The CD19 signal transduction molecule is a response regulator of B-lymphocyte differentiation. *Proc Natl Acad Sci U S A.* 1995;92:11558–11562. doi:10.1073/pnas.92.25.11558.
17. Inaoki M, Sato S, Weintraub BC, Goodnow CC, Tedder TF. CD19-regulated signaling thresholds control peripheral tolerance and autoantibody production in B lymphocytes. *J Exp Med.* 1997;186:1923–1931. doi:10.1084/jem.186.11.1923.
18. Saito E, Fujimoto M, Hasegawa M, Komura K, Hamaguchi Y, Kaburagi Y, Nagaoka T, Takehara K, Tedder TF, Sato S. CD19-dependent B lymphocyte signaling thresholds influence skin fibrosis and autoimmunity in the tight-skin mouse. *J Clin Invest.* 2002;109:1453–1462. doi:10.1172/JCI15078.
19. Hammer O. CD19 as an attractive target for antibody-based therapy. *MAbs.* 2012;4:571–577. doi:10.4161/mabs.21338.
20. Callard RE, Rigley KP, Smith SH, Thurstan S, Shields JG. CD19 regulation of human B cell responses. B-cell proliferation and antibody secretion are inhibited or enhanced by ligation of the CD19 surface glycoprotein depending on the stimulating signal used. *J Immunol.* 1992;148:2983–2987.
21. Pezzutto A, Dorken B, Rabinovitch PS, Ledbetter JA, Moldenhauer G, Clark EA. CD19 monoclonal antibody HD37 inhibits anti-immunoglobulin-induced B-cell activation and proliferation. *J Immunol.* 1987;138:2793–2799.
22. Rigley KP, Callard RE. Inhibition of B-cell proliferation with anti-CD19 monoclonal antibodies: anti-CD19 antibodies do not interfere with early signaling events triggered by anti-IgM or interleukin 4. *Eur J Immunol.* 1991;21:535–540. doi:10.1002/eji.1830210302.
23. Buatois V, Johnson Z, Salgado-Pires S, Papaioannou A, Hatterer E, Chauchet X, Richard F, Barba L, Daubeuf B, Cons L, et al. Preclinical development of a bispecific antibody that safely and effectively targets CD19 and CD47 for the treatment of B-Cell lymphoma and leukemia. *Mol Cancer Ther.* 2018;17:1739–1751. doi:10.1158/1535-7163.MCT-17-1095.
24. Xu L, Li G, Wang J, Fan Y, Wan Z, Zhang S, Shaheen S, Li J, Wang L, Yue C, et al. Through an ITIM-independent mechanism the FcγRIIB blocks B cell activation by disrupting the colocalized microclustering of the B cell receptor and CD19. *J Immunol.* 2014;192:5179–5191. doi:10.4049/jimmunol.1400101.
25. Breton CS, Nahimana A, Aubry D, Maccin J, Moretti P, Bertschinger M, Hou S, Duchosal MA, Back J. A novel anti-CD19 monoclonal antibody (GBR 401) with high killing activity against B cell malignancies. *J Hematol Oncol.* 2014;7:33. doi:10.1186/1756-8722-7-33.
26. Yanaba K, Bouaziz JD, Matsushita T, Magro CM, St Clair EW, Tedder TF. B-lymphocyte contributions to human autoimmune disease. *Immunol Rev.* 2008;223:284–299. doi:10.1111/j.1600-065X.2008.00646.x.
27. Cherukuri A, Cheng PC, Sohn HW, Pierce SK. The CD19/CD21 complex functions to prolong B cell antigen receptor signaling from lipid rafts. *Immunity.* 2001;14:169–179. doi:10.1016/S1074-7613(01)00098-X.
28. de W, I, Koopmans SM, Kater AP, van GM. Incidence and management of toxicity associated with ibrutinib and idelalisib: a practical approach. *Haematologica.* 2017;102:1629–1639. doi:10.3324/haematol.2017.164103.
29. Stolz C, Schuler M. Molecular mechanisms of resistance to Rituximab and pharmacologic strategies for its circumvention. *Leuk Lymphoma.* 2009;50:873–885. doi:10.1080/10428190902878471.
30. Weiner GJ. Rituximab: mechanism of action. *Semin Hematol.* 2010;47:115–123. doi:10.1053/j.seminhematol.2010.01.011.
31. Chao MP, Alizadeh AA, Tang C, Myklebust JH, Varghese B, Gill S, Jan M, Cha AC, Chan CK, Tan BT, et al. Anti-CD47 antibody synergizes with rituximab to promote phagocytosis and eradicate non-Hodgkin lymphoma. *Cell.* 2010;142:699–713. doi:10.1016/j.cell.2010.07.044.
32. Davis TA, Czerwinski DK, Levy R. Therapy of B-cell lymphoma with anti-CD20 antibodies can result in the loss of CD20 antigen expression. *Clin Cancer Res.* 1999;5:611–615.
33. Gallagher S, Turman S, Lekstrom K, Wilson S, Herbst R, Wang Y. CD47 limits antibody dependent phagocytosis against non-malignant B cells. *Mol Immunol.* 2017;85:57–65. doi:10.1016/j.molimm.2017.01.022.
34. Karnell JL, Dimasi N, Karnell FG III, Fleming R, Kuta E, Wilson M, Wu H, Gao C, Herbst R, Ettinger R. CD19 and CD32b differentially regulate human B cell responsiveness. *J Immunol.* 2014;192:1480–1490. doi:10.4049/jimmunol.1301361.
35. Pulczynski S. Antibody-induced modulation and intracellular transport of CD10 and CD19 antigens in human malignant B cells. *Leuk Lymphoma.* 1994;15:243–252. doi:10.3109/10428199409049720.
36. Mattila PK, Feest C, Depoil D, Treanor B, Montaner B, Otipoby KL, Carter R, Justement LB, Bruckbauer A, Batista FD. The actin and tetraspanin networks organize receptor nanoclusters to regulate B cell receptor-mediated signaling. *Immunity.* 2013;38:461–474. doi:10.1016/j.immuni.2012.11.019.

37. Dahl KN, Westhoff CM, Discher DE. Fractional attachment of CD47 (IAP) to the erythrocyte cytoskeleton and visual colocalization with Rh protein complexes. *Blood*. 2003;101:1194–1199. doi:10.1182/blood-2002-04-1187.
38. Mouro-Chanteloup I, Delaunay J, Gane P, Nicolas V, Johansen M, Brown EJ, Peters LL, Van Kim CL, Cartron JP, Colin Y. Evidence that the red cell skeleton protein 4.2 interacts with the Rh membrane complex member CD47. *Blood*. 2003;101:338–344. doi:10.1182/blood-2002-04-1285.
39. Li X, Carter RH. Convergence of CD19 and B cell antigen receptor signals at MEK1 in the ERK2 activation cascade. *J Immunol*. 1998;161:5901–5908.
40. Kawasaki Y, Senda T, Ishidate T, Koyama R, Morishita T, Iwayama Y, Higuchi O, Akiyama T. Asef, a link between the tumor suppressor APC and G-protein signaling. *Science*. 2000;289:1194–1197. doi:10.1126/science.289.5482.1194.
41. Mizuno N, Narita A, Kon T, Sutoh K, Kikkawa M. Three-dimensional structure of cytoplasmic dynein bound to microtubules. *Proc Natl Acad Sci U S A*. 2007;104:20832–20837. doi:10.1073/pnas.0710406105.
42. Nagata K, Inagaki M. Cytoskeletal modification of Rho guanine nucleotide exchange factor activity: identification of a Rho guanine nucleotide exchange factor as a binding partner for Sept9b, a mammalian septin. *Oncogene*. 2005;24:65–76. doi:10.1038/sj.onc.1208101.
43. Padovano V, Lucibello I, Alari V, Della MP, Crespi A, Ferrari I, Recagni M, Lattuada D, Righi M, Toniolo D, et al. The POF1B candidate gene for premature ovarian failure regulates epithelial polarity. *J Cell Sci*. 2011;124:3356–3368. doi:10.1242/jcs.088237.
44. Ghetie MA, Picker LJ, Richardson JA, Tucker K, Uhr JW, Vitetta ES. Anti-CD19 inhibits the growth of human B-cell tumor lines in vitro and of Daudi cells in SCID mice by inducing cell cycle arrest. *Blood*. 1994;83:1329–1336.
45. Fleire SJ, Goldman JP, Carrasco YR, Weber M, Bray D, Batista FD. B cell ligand discrimination through a spreading and contraction response. *Science*. 2006;312:738–741. doi:10.1126/science.1123940.
46. Song W, Liu C, Upadhyaya A. The pivotal position of the actin cytoskeleton in the initiation and regulation of B cell receptor activation. *Biochim Biophys Acta*. 2014;1838:569–578. doi:10.1016/j.bbame.2013.07.016.
47. Treanor B, Depoil D, Gonzalez-Granja A, Barral P, Weber M, Dushek O, Bruckbauer A, Batista FD. The membrane skeleton controls diffusion dynamics and signaling through the B cell receptor. *Immunity*. 2010;32:187–199. doi:10.1016/j.immuni.2009.12.005.
48. Treanor B, Depoil D, Bruckbauer A, Batista FD. Dynamic cortical actin remodeling by ERM proteins controls BCR microcluster organization and integrity. *J Exp Med*. 2011;208:1055–1068. doi:10.1084/jem.20101125.
49. Fischer N, Elson G, Magistrelli G, Dheilily E, Fouque N, Lauredon A, Gueneau F, Ravn U, Depoisier JF, Moine V, et al. Exploiting light chains for the scalable generation and platform purification of native human bispecific IgG. *Nat Commun*. 2015;6:6113. doi:10.1038/ncomms7113.
50. Walshe CA, Beers SA, French RR, Chan CH, Johnson PW, Packham GK, Glennie MJ, Cragg MS. Induction of cytosolic calcium flux by CD20 is dependent upon B Cell antigen receptor signaling. *J Biol Chem*. 2008;283(20):16971. doi:10.1074/jbc.M708459200.